ORIGINAL ARTICLE

Different effects of tropical cyclones generated in the South China Sea and the northwest Pacific on the summer South China Sea circulation

Zheng Ling · Guihua Wang · Chunzai Wang · Zhi-Song Fan

Abstract Tropical cyclones (TCs) that affect the South China Sea (SCS) can be generated in either the SCS or the northwestern Pacific (NWP). Using satellite measurements, the Sverdrup theory and a 1.5-layer nonlinear reduced gravity model, the present paper investigates the effects of SCS and NWP TCs on the summer SCS upper layer ocean circulation. Both SCS and NWP TCs enhance the summer mean circulation pattern of the cyclonic gyre in the northern SCS and the anti-cyclonic gyre in the southern SCS. However, the effect of SCS TCs is much larger than that of NWP TCs, although the number of SCS TCs is smaller than NWP TCs. This is because the SCS TCs-induced wind stress curl pattern is favorable for enhancing the summer SCS mean circulation.

Keywords Upper layer circulation · Tropical cyclones · South China Sea · The northwestern Pacific

1 Introduction

The South China Sea (SCS) is a semi-enclosed ocean basin temporally forced by the pronounced monsoon wind. The

Z. Ling · Z.-S. Fan
College of Physical and Environmental Oceanography,
Ocean University of China, Qingdao, China

Z. Ling · G. Wang (✉)
State Key Laboratory of Satellite Ocean Environment Dynamics,
Second Institute of Oceanography, SOA, Hangzhou, China
e-mail: guihua_wanggh@yahoo.com.cn

C. Wang
Physical Oceanography Division, NOAA/Atlantic
Oceanographic and Meteorological Laboratory,
Miami, FL, USA

southwesterly and northeasterly winds prevail in the SCS in summer and winter, respectively. The southwesterly wind usually occurs around mid-May in the southern and central SCS, then expands to the entire SCS in June, and matures from July to August. The strong northeasterly winter monsoon first appears over its northern part in September, reaching its central part in October and covering the entire SCS in November, and then gradually diminishing in April.

The SCS is also an ocean basin that is often affected by tropical cyclones (TCs) generated either over the northwestern Pacific (NWP) or the SCS (Wang et al. 2007). As in many studies, we define TC as a tropical mesoscale cyclonic weather system with its strength of a tropical storm or stronger (i.e., typhoon). Our TC dataset shows that, among the summer (winter) average of 5.3 (3) TCs passing through the SCS, about 1.5 (0.25) TCs are originated or generated within the SCS and the remaining TCs are originated from the NWP.

Since large-scale upper layer ocean circulation in the SCS is mainly driven by the surface wind, both the monsoon-related and TC-induced winds should play a role in SCS circulation. How the SCS upper layer responds to the monsoon has been well studied (Liu et al. 2001; Wang et al. 2006). It has been shown that a winter basin-wide cyclonic gyre with two cyclonic cells is forced by the winter monsoon, while a weakened cyclonic gyre north of about 12°N and a strong anti-cyclonic gyre south of about 12°N are produced by the summer monsoon. Associated with these gyres are strong western boundary currents. In winter, a southward jet flows along the entire western boundary (Wrytki 1961; Liu et al. 2001; Wang et al. 2008). In summer, there is a northward jet flowing along the western boundary in the southern SCS (Xu et al. 1982). The jet apparently veers eastward off central Vietnam near 12°N (Xu et al. 1982; Xie et al. 2003; Wang et al. 2003,

2006). To the north, there is a narrow southwestern jet along the continental slope in the northwest SCS (Qu 2000; Metzger and Hurlburt 2001; Su 2004).

However, there are few studies that have examined the SCS response to TC-induced wind. Chu et al. (1999) used the Princeton Ocean Model to investigate the SCS response to TC 'Ernie' and studied the sea surface temperature cooling to the right of TC track and a very strong divergent upper layer current. Lin et al. (2003) combined several datasets to show the effects of TCs on chlorophyll and marine life. Recently, Wang et al. (2009) investigated the seasonal variability of SCS ocean circulation induced by TCs using satellite QuikSCAT wind field data and a reduced gravity model. They found that TCs can affect both large-scale and mesoscale SCS ocean circulation. As stated earlier, TCs that affect the SCS can be formed in either the SCS or the NWP. However, whether TCs generated in the SCS and the NWP have different effects on SCS circulation is unknown. The purpose of the present paper is to answer and address this question. Because there are few SCS TCs during the northeasterly monsoon period, as shown in Table 1, NWP TCs dominate the influence of TCs on the mean SCS circulation with an enhancement of the basin-wide cyclonic flow in this period. Thus, this study will focus on different effects of TCs generated in the SCS and the NWP on the summer SCS circulation during the southwesterly monsoon period.

We will first use the QuikSCAT wind, one of the best wind products available, to estimate the wind stress curls induced by SCS and NWP generated TCs. A simple model of the Sverdrup theory and a 1.5-layer reduced gravity model are then used to investigate the effects of TCs generated in the SCS and NWP on SCS ocean circulation.

2 Data

The TC dataset is from the Japanese Meteorological Agency. The cover period of the dataset is from January 2000 to December 2007. The starting year of 2000 is chosen because it is the beginning of a complete year for the QuikSCAT wind data. The TC dataset includes 6-hourly positions of each TC, its impact radius, and its associated minimum center pressure and maximum wind

speed. We choose all TCs that could have an impact on the SCS, defined for this purpose as the area of 0–22.5°N, 98.5–120.5°E.

The QuikSCAT wind dataset we used is from the Jet Propulsion Laboratory. The spatial resolution of Quik-SCAT wind dataset is 0.25° latitude by 0.25° longitude and the time resolution is 1 day. To evaluate the QuikSCAT wind data quality, we compared the QuikSCAT wind in the SCS with the observed winds from two islands during May 2005–December 2006. The root mean square errors between the QuikSCAT and island observations for wind speed and wind direction are 1.65 m/s and 27.8°, respectively. These values are consistent with the results of Liu and He (2003) who compared the QuikSCAT wind in the SCS with the observed wind on seven islands. As demonstrated in previous studies, the QuikSCAT wind over the SCS is useful to simulate SCS circulation (Xie et al. 2003; Wang et al. 2006, 2008), although the QuikSCAT wind shows some differences from island observed wind.

To examine the effect of TCs on SCS ocean circulation, we reconstructed four sets of wind products from the QuikSCAT wind dataset as follows:

A. The original QuikSCAT wind data.
B. The wind data excluding all TCs.
C. The wind data excluding TCs generated over the NWP.
D. The wind data excluding TCs generated over the SCS.

Hereinafter, we will use A, B, C and D to denote the four wind forcings, respectively. Note that a simple linear interpolation in time is used to reconstruct the wind forcing for those periods during which we exclude TCs. For example, if a TC occurs from 6 to 8 June, we remove the 3 days' original wind fields first, and then use the wind field on 5 and 9 June to obtain the wind field for the removed 3 days with the linear interpolation method. The simple method is very effective in excluding TCs, but leaving the background wind field (the monsoon wind).

A multiple altimeter dataset from the US Naval Research Laboratory, derived from TOPEX/POSEIDON, Jason, ERS and Geosat Follow-On (GFO), is used to validate our model results. The spatial resolution of the dataset is 0.25° × 0.25° and the time resolution is daily within the period from year 2000 to 2007.

Table 1 The number of tropical cyclones which affect the South China Sea from 2000 to 2007

Month	Jan	Feb	Mar	Apr	May	Jun	Jul	Aug	Sep	Oct	Nov	Dec
SCS tropical cyclones	0	0	0	0	4	3	4	6	5	1	0	1
NWP tropical cyclones	0	0	1	1	2	5	11	13	9	7	12	3
Total	0	0	1	1	6	8	15	19	14	8	12	4

3 Methods

3.1 Sverdrup theory

The Sverdrup theory is a primary balance for the large-scale wind-driven ocean circulation (Sverdrup 1947). Many studies have applied it to calculate the large-scale circulations in the Pacific, Atlantic and Indian Oceans. This simple model has also been successfully applied to study SCS circulation (Metzger and Hurlburt 1996; Shaw et al. 1999; Liu et al. 2001). The wind-driven transport stream-function (ψ) for flow integrated in the entire water column can be estimated by the Sverdrup theory as:

$$\psi(x) = -\frac{1}{\rho\beta}\int_{x}^{x_E} curl(\tau)dx,$$

where ρ is the density of the water, β is the northward gradient of the planetary vorticity, and x_E represents the ocean eastern boundary. The boundary condition is $\psi = 0$ at x_E.

The curl of wind stress (τ) in the Sverdrup relation can be calculated by the following formula:

$$curl(\tau) = \frac{\partial\tau_y}{\partial x} - \frac{\partial\tau_x}{\partial y}.$$

The zonal and meridional wind stress τ_x and τ_y in the above equation can be obtained as:

$$\tau_x = \rho_a C_D |V| u$$
$$\tau_y = \rho_a C_D |V| v$$
$$C_D = \begin{cases} 0.0012, & |V| < 11 \\ (0.45 + 0.069 \times |V|) \times 0.001, & |V| < 11, \end{cases}$$

where C_D is the wind stress drag coefficient (Yin et al. 2007), ρ_a is the density of air; $|V|$ is the wind speed, u is the zonal wind, and v is the meridional wind. We use the monthly wind to drive the Sverdrup model. Thus, we define the summer mean is the average of the monthly dataset from June to August for the Sverdrup model output.

3.2 Reduced gravity model

A 1.5-layer nonlinear reduced gravity model is also employed to simulate the wind-driven upper ocean circulation. Our model boundary is along the 200-m isobaths (Fig. 1). The reduced gravity is set to 0.03 m s^{-2}, with the lateral friction coefficient of 500 m^2 s^{-1} and the initial thermocline depth of 200 m. The model resolution is on a grid of 0.25° latitude by 0.25° longitude. The grid size is smaller than the first baroclinic Rossby radius of deformation for the deep basin of the SCS, which is larger than 50 km (Cai et al. 2008). The model is spun up with the
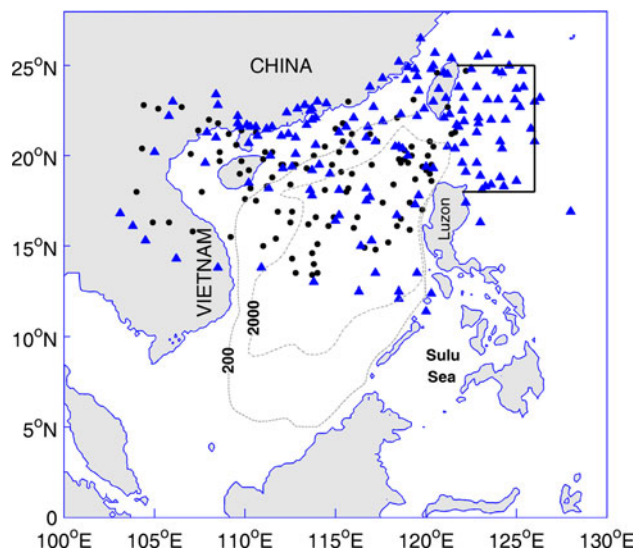
Fig. 1 The SCS and the 12-h locations of TCs in summer (*triangles* represent NWP TCs and *solid circles* represent SCS TCs). The two isobaths are for 200 and 2,000 m, respectively. The open ocean boundaries are set at 18°N and 24.5°N lines, and the boundary along 126°E is set as a wall

winds switched on gradually from rest to the wind distribution of 1 January 2000 over a 1-month period. The model is then run with the wind forcing data of the whole year from 1 January to 31 December 2000. The model run is repeated for 4 years until the ocean circulation reaches a quasi-equilibrium state. Then, the model is forced from 1 January 2000 to 31 December 2007 with the four wind forcings of A, B, C, and D as mentioned in Sect. 2. More details of this simple model can be found in Wang et al. (2006, 2008, 2009). The reduced gravity model output is daily, and we thus define the summer mean as the average of the daily dataset from 1 June to 31 August.

To include the Kuroshio as a driving force in some experiments, we open the Luzon Strait and specify a Kuroshio input along the zonal section of 122–124.5°E (18°N). The open boundary conditions are given, as done by Hurlburt and Thompson (1980). The idea of the open boundary conditions is that: the profile of transport is prescribed for inflow at south and the normal flow at the north port is self-determined with the integral constraint that the total transport of outflow matches the inflow, and the amplitude of the tangential component is set to zero one-half grid distance outside the physical domain at both south and north ports. A natural question is whether the set of open boundary conditions can produce more realistic simulations than the close boundary conditions. Figure 2a–c show the summer empirical orthogonal function (EOF) modes of MODAS sea surface height anomaly (SSHA) and the simulated thermocline depth anomaly with two experiments (including the Kuroshio and excluding the Kuroshio). It should be noted that these modes are mainly
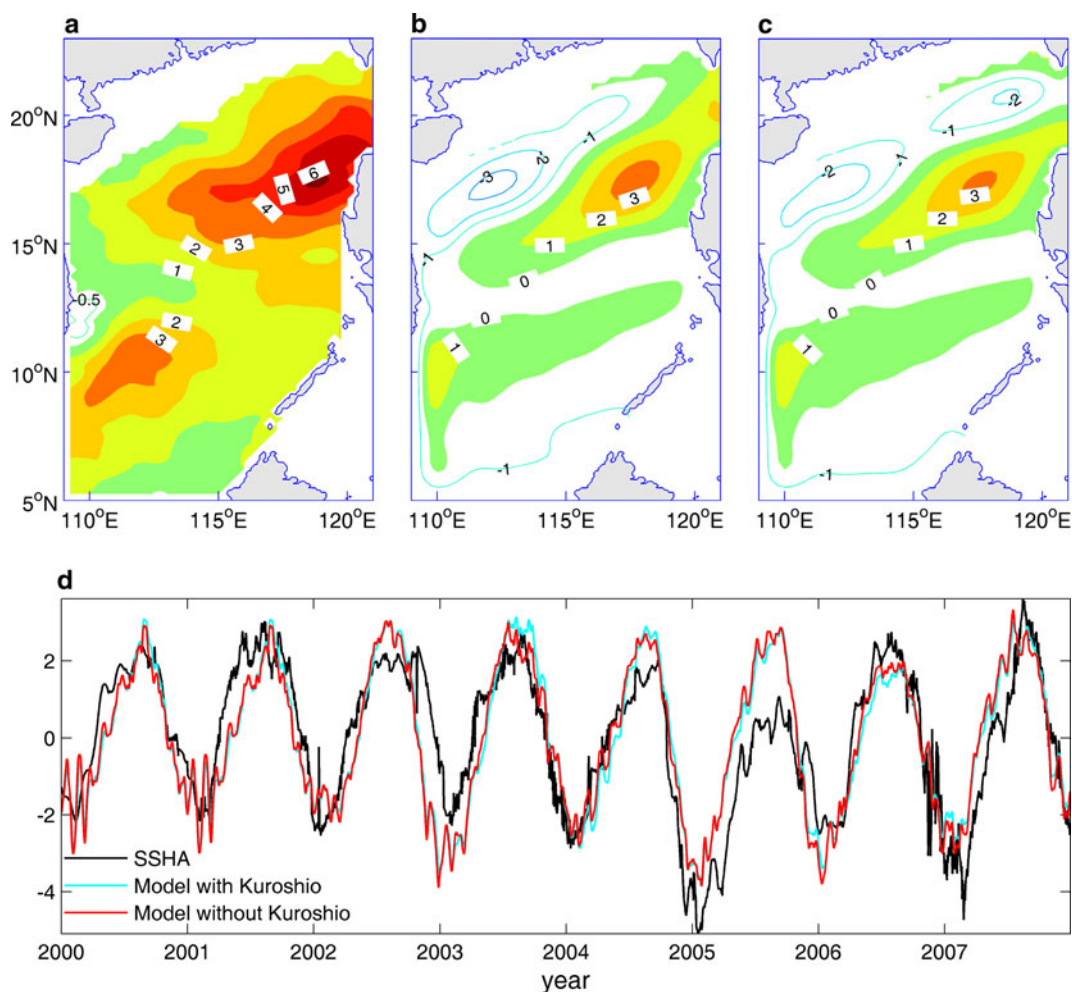
Fig. 2 EOF summer mode of **a** the SSHA (cm), **b** the modeled thermocline depth anomaly (m) with the Kuroshio, and **c** the modeled thermocline depth anomaly (m) without the Kuroshio; **d** their corresponding time series

reflecting summer circulation although the principal components (PCs) show a robust seasonal variability. The summer modes account for 49.7%, 43.9% and 40.9% of total variance for MODAS SSHA, the thermocline depth anomalies including Kuroshio and excluding the Kuroshio, respectively. The MODAS SSHA shows that there is an anti-cyclonic anomaly south of 12°N, a cyclonic anomaly in the northwestern SCS and another anti-cyclonic anomaly northwest of Luzon Island. The patterns of the two simulated thermocline depth anomaly are generally similar to MODAS SSHA (a northern cyclonic gyre and a southern anti-cyclonic gyre driven by the monsoon). The correlation is 0.82 between the observed PC and the simulated PC excluding the Kuroshio. The correlation is 0.84 (slightly higher) for the case including the Kuroshio. This suggests that the open boundary condition for including the Kuroshio can slightly help by having more accurate simulations. The validity and effectiveness of such a simple model to study the SCS circulation dynamics over the deep water

have also been demonstrated by many other studies (e.g., Metzger and Hurlburt 1996; Liu et al. 2001; Wang et al. 2006, 2008).

4 Results

4.1 Sverdrup relationship

From 2000 to 2007, there were 42 TCs in summer that affected the SCS. Of these 42 TCs, 13 were generated over the SCS and the other 29 were formed in the NWP (Table 1). Figure 1 shows the 12-h positions of the 42 TCs, all of which were located to the north of 12°N.
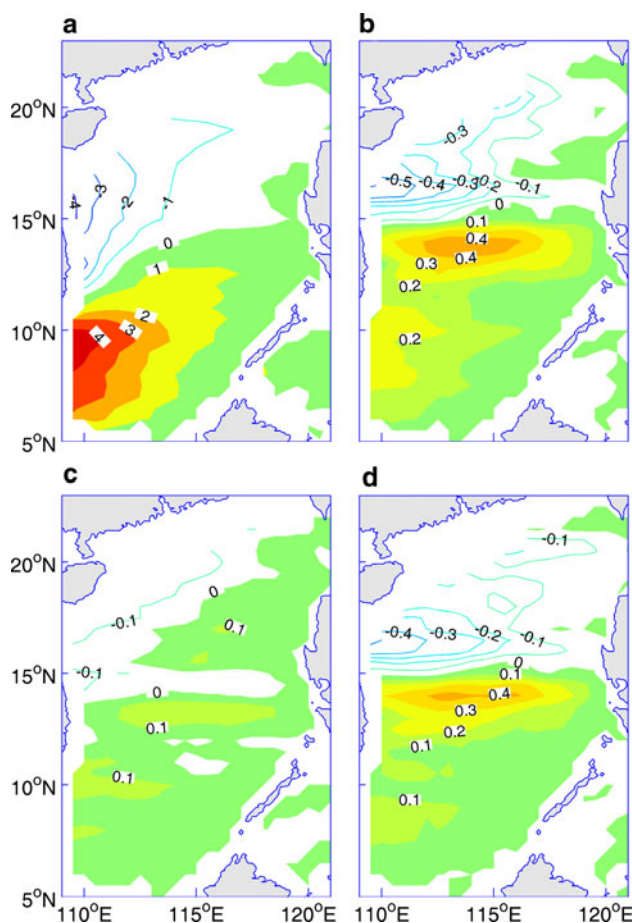
In summer, the southwest monsoon induces positive (negative) wind stress curl in the northwestern (southeastern) SCS (Fig. 3a). Figure 3b shows that the TCs in summer induce a larger positive wind stress curl in the northwestern SCS and negative wind stress curl in the
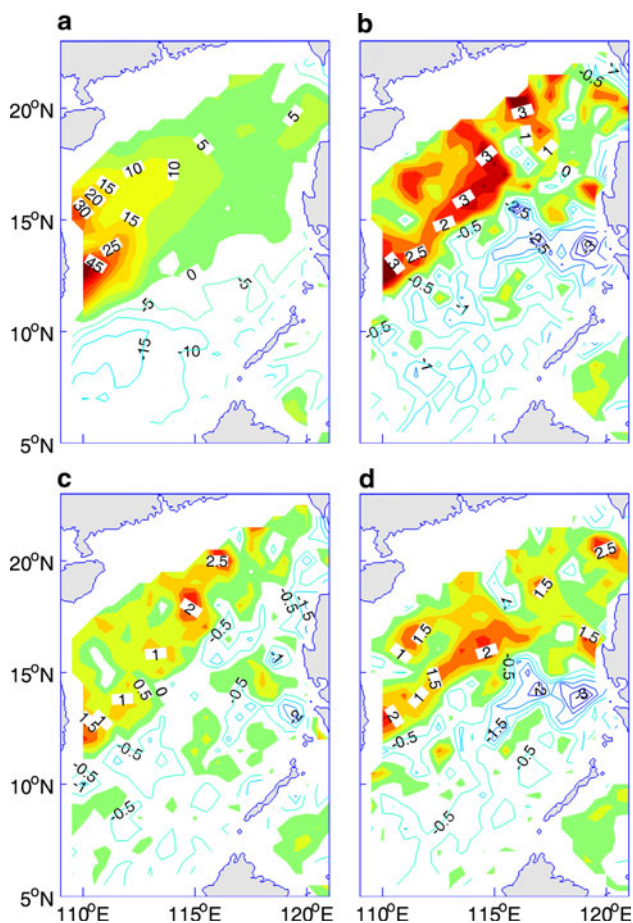
Fig. 3 TC-induced wind stress curls (10^{-8} N m^{-3}) in summer. **a** The wind stress curl of the original wind forcing, **b** the wind stress curl difference between the original wind forcing and the wind forcing without any TCs, **c** the wind stress curl difference between the wind forcing only with NWP TCs and the wind forcing without any TCs, and **d** the wind stress curl difference between the wind forcing only with SCS TCs and the wind forcing without any TCs. The positive values are *shaded*

Fig. 4 Stream function (Sv 10^6 m^3 s^{-1}) calculated from the Sverdrup theory in summer. **a** Mean stream function forced by the original wind, **b** stream function difference between the original wind forcing and the wind forcing without any TCs, **c** stream function difference between the wind forcing only with NWP TCs and the wind forcing without any TCs, and **d** stream function difference between the wind forcing only with SCS TCs and the wind forcing without any TCs. The positive values are *shaded*

southeastern SCS. Although the general pattern of wind stress curl induced by NWP TCs is similar to that induced by SCS TCs (Fig. 3c, d), there are some distinguished differences. The positive wind stress curl induced by SCS TCs is north of 15°N, whereas the positive wind stress curl induced by NWP TCs retreats northwestward with a relatively small band of the positive curl. Interestingly, for the case of the NWP TC-induced wind stress curl, a negative wind stress curl appears in the northwest of Luzon Island (Fig. 3c).

The summer SCS ocean circulation is dominated by double gyres: a north cyclonic gyre and a south anti-cyclonic gyre (Fig. 4a). Because TCs produce a positive and negative wind stress curl in the northwestern and southeastern SCS, respectively (Fig. 3b), the TC-induced Sverdrup stream function also shows a north cyclonic gyre and a south anti-cyclonic gyre (Fig. 4b). Note that we

obtain the TC-induced Sverdrup stream function through the difference among large-scale circulations (Sverdrup stream functions) forced by the wind field described in Sect. 2, not through TC wind driven directly. Figure 4b indicates that TCs enhances both the cyclonic and anti-cyclonic gyres in summer. As shown in Fig. 4c, d, both NWP and SCS TCs can enhance the double gyre circulation. However, the effect of SCS TCs is much larger than that of NWP TCs, although the number of NWP TCs in summer is larger than SCS TCs. This is because the wind stress curl pattern induced by SCS TCs is more favorable for increasing the Sverdrup stream function than NWP TCs (Fig. 3c, d). There are two reasons why SCS TCs produce more favorable wind stress curl pattern than NWP TCs. Firstly, the distribution of TCs shows that some NWP TCs are located in the northeastern SCS, whereas most SCS TCs are in the central SCS (Fig. 1). When a NWP TC
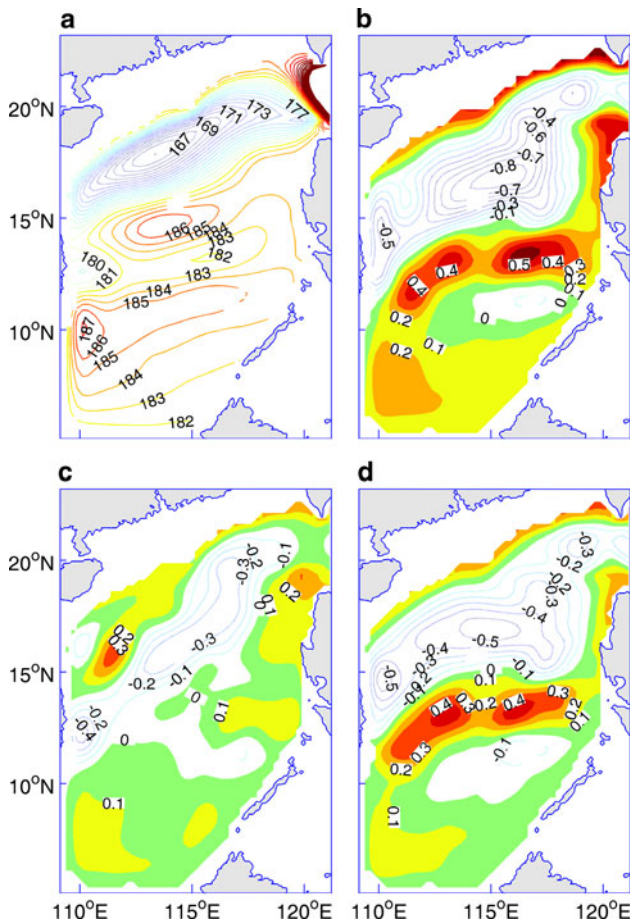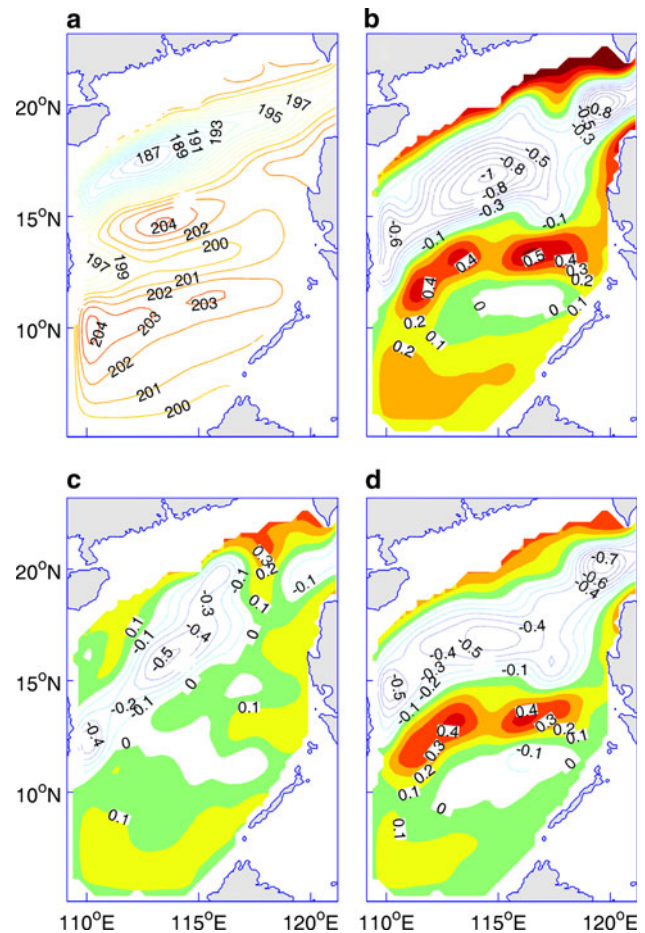
Fig. 5 Thermocline depth (m) in summer from the model experiment with the Kuroshio. **a** Mean thermocline depth forced by the original wind, **b** thermocline depth difference between the original wind forcing and the wind forcing without any TCs, **c** thermocline depth difference between the wind forcing only with NWP TCs and the wind forcing without any TCs, and **d** stream function difference between the wind forcing only with SCS TCs and the wind forcing without any TCs. **a** The *dashed* (*solid*) contours are for the thermocline depth smaller (larger) than 182 m. **b–d** The positive values are *shaded*

Fig. 6 The same as Fig. 5, except for the model experiment without the Kuroshio. **a** The *dashed* (*solid*) contours are for the thermocline depth smaller (larger) than 200 m. **b–d** The positive values are *shaded*

passes the northeastern SCS, it will induce a negative wind stress curl there, which is unfavorable for enhancing the cyclonic gyre in the northern SCS. Secondly, the time that SCS TCs are centered over the SCS basin (109–121°E, 5°N–23°N) is longer than that of NWP TCs, at 43.5 and 37.5 days, respectively, during summer for the period from 2000 to 2007. This indicates that SCS TCs may produce more positive wind stress curl in the SCS.

4.2 Reduced gravity model

The Sverdrup theory assumes that the ocean is in near-equilibrium with surface wind forcing and neglects the details of ocean adjustment. To consider the ocean adjustment processes and more complete ocean processes,

we conduct a series of 1.5-layer reduced gravity model experiments to further investigate how NWP and SCS TCs affect summer SCS circulation. We use the four wind datasets of A, B, C and D discussed in Sect. 2 to drive the model with open boundary conditions.

Figure 5a shows the modeled summer mean thermocline depth over the SCS from 2000 to 2007. The summer mean circulation pattern includes a cyclonic gyre north of 12°N and an anti-cyclonic gyre south of 12°N. Associated with these two gyres, a dipole structure of oceanic eddy appears off central Vietnam with a cyclonic eddy north and an anti-cyclonic eddy south (note that an eastward jet is between the dipole eddies; Liu et al. 2001; Wang et al. 2010). The model run also demonstrates that TCs can enhance the cyclonic gyre in the northern SCS and an anti-cyclonic gyre in the southern SCS (Fig. 5b). The pattern of the summer thermocline depth induced by NWP and SCS TCs are similar (Fig. 5c, d), with both the cyclonic and anti-cyclonic gyres being enhanced. However, as demonstrated by the Sverdrup theory in the last section, the enhancement

by SCS TCs is stronger than that by NWP TCs. As expected, the dipole structure of an anti-cyclonic eddy south of an eastward jet and a cyclonic eddy north is more intensified by SCS TCs than NWP TCs.

To examine the effect of the boundary condition, we use the same four wind datasets mentioned above to drive the model except with a close boundary (without the Kuroshio's effect). As shown in Fig. 6a, the modeled circulation pattern without the Kuroshio is generally similar to that with the open boundary condition, except in the area near Luzon Strait (Fig. 5a). The result is consistent with the previous studies that showed that the SCS circulation is mainly driven by the monsoon (Liu et al. 2001; Wang et al. 2006). The TCs-induced circulation patterns with the close boundary condition (Fig. 6b–d) are also similar to those with the open boundary condition (Fig. 5b–d). All of them show that both the cyclonic gyre and the anti-cyclonic gyre are enhanced by the TCs. However, the TCs-induced cyclonic circulation in the north with the close boundary condition is slightly stronger than that with the open boundary condition (Figs. 5b and 6b), suggesting that interaction between TCs and the Kuroshio can produce a negative vorticity.

Since the model includes the nonlinear terms, it will be valuable to evaluate the nonlinear effect on the TCs-induced circulation. We use the same four wind forcing datasets to drive the model excluding the nonlinear terms. As shown in Fig. 7, the Kuroshio can intrude into the SCS if the nonlinear terms are excluded, which is consistent with previous model results (Zhang et al. 2006). Except for the anti-cyclonic gyre in the northeastern SCS, the SCS circulation also includes a cyclonic gyre in the north and an anti-cyclonic gyre in the south. It is interesting to note that both the north cyclonic gyre and the south anti-cyclonic gyre are still enhanced by the TCs, although the nonlinear terms are excluded. This suggests that the nonlinear terms are not important to the TCs-induced circulation, in spite of its significant impact on the Kuroshio intrusion.

All of the modeled results are qualitatively consistent with the Sverdrup theory. Both SCS and NWP TCs can enhance the SCS double gyres in summer. Although the number of NWP TCs is much larger than that of the SCS, the effect of NWP TCs on the summer SCS circulation gyres is weaker than that of SCS TCs. This is because the positive wind stress curl induced by NWP TCs is more northwestward than SCS TCs, and NWP TCs produce a negative wind stress curl in the northwest of Luzon Islands.

The available navy daily satellite SSHA dataset is used to verify the model results. Since the inertial oscillation induced by TC in SCS can last 6–8 days after the TC passage (Zhu and Li 2007), we define the difference of the SSHA between 1 day before the TC passage and 7 days after the TC passage as the SSHA difference induced by TCs. As shown
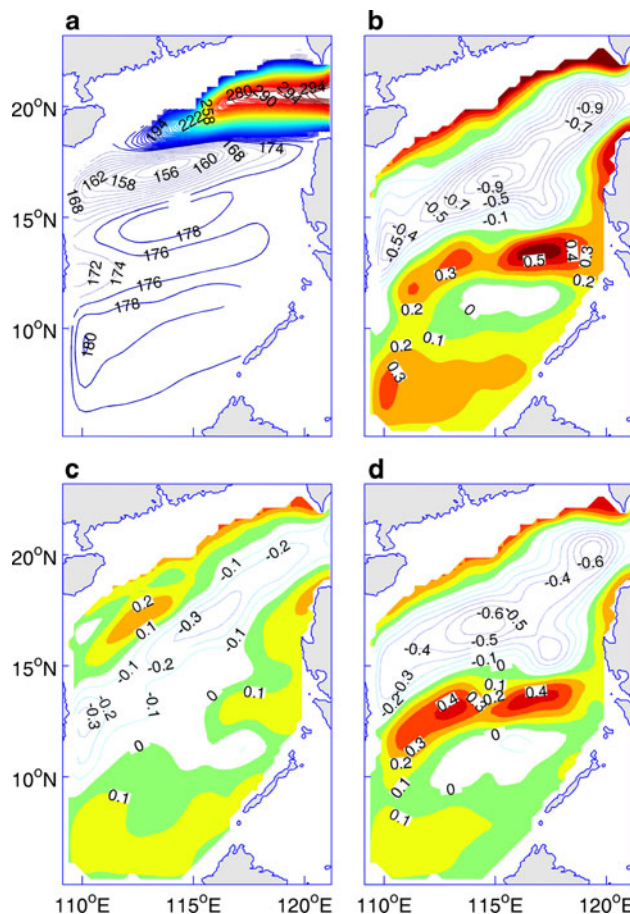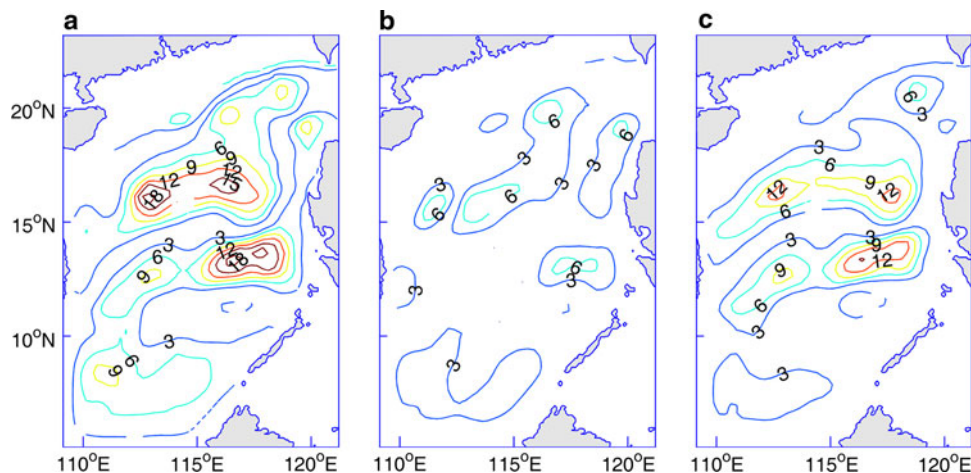

Fig. 7 The same as Fig. 5, except for the model experiment without the nonlinear effect. **a** The *dashed* (*solid*) contours are for the thermocline depth smaller (larger) than 175 m. **b–d** The positive values are *shaded*
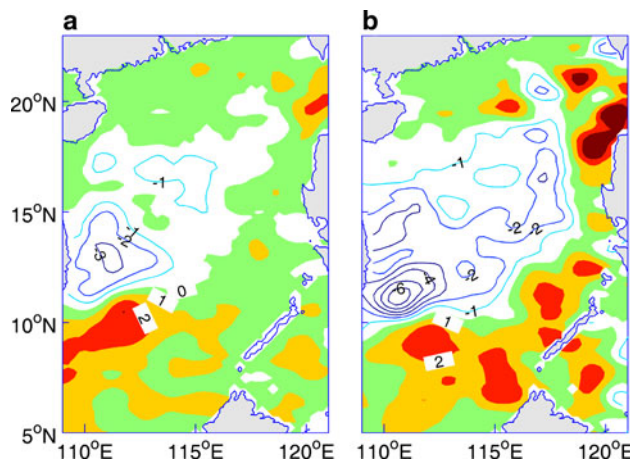
Fig. 8 The summer averaged SSHA (cm) induced by **a** NWP TCs and **b** SCS TCs

in Fig. 8, both NWP TCs and SCS TCs can enhance the northern cyclonic gyre and the southern anti-cyclonic gyre. The dipole off central Vietnam is also much intensified by the

two types of TCs. It is also shown that SCS TCs can induce a stronger double gyres than NWP TCs. All these are consistent with the models' results described above, giving confidence in the results presented in this paper.

5 Summary and discussion

This study shows that the wind stress curl induced by TCs generated either over the NWP or the SCS can affect the summer SCS ocean circulation. In summer, both NWP and SCS TCs tend to enhance the summer circulation pattern of the cyclonic gyre in the northern SCS and the anti-cyclonic gyre in the southern SCS. However, the relative importance of NWP and SCS TCs in the summer SCS circulation is different. The effect of SCS TCs on summer SCS circulation is much larger than that of NWP TCs although the number of SCS TCs is smaller than NWP TCs. This is because the SCS TCs-induced wind stress curl pattern is more favorable for enhancing the summer SCS circulation pattern. Generally speaking, neither the Kuroshio effect nor the nonlinear effect are sufficiently significant to affect the TCs-induced summer circulation.

To evaluate the contribution of the TC-induced circulation, we calculated the ratio between the TC-induced summer thermocline depth variance and the magnitude of the summer thermocline depth variability, as shown in Fig. 9. All TCs can contribute about 0–18% of the original circulation (Fig. 9a). The SCS and NWP contributions are about 0–12% and 0–6%, respectively (Fig. 9b, c). These values indicate that the TC influence is an important factor in affecting SCS upper layer circulation and that the contribution by TCs generated in the SCS is larger than those in the NWP.

As stated in the "Introduction", most SCS studies do not consider the effect of TC-induced wind forcing on the SCS. The present paper uses the simple Sverdrup theory and a

reduced gravity model as well as observations to show that both TCs generated in the SCS and in the NWP play an important role in the summer SCS ocean circulation. This suggests that a complete understanding of SCS ocean circulation requires us to consider and include the TCs' influence. In addition, more complicated ocean general circulation models are needed to investigate the effect of TCs on SCS ocean circulation.

References

Chu PC, Lv SH, Liu WT (1999) Uncertainty of the South China Sea prediction using NSCAT and NCEP winds during tropical storm Ernie 1996. J Geophys Res 104:11273–11289

Cai SQ, Long XM, Wu RH, Wang SG (2008) Geographical and monthly variability of the first baroclinic Rossby radius of deformation in South China Sea. J Mar Syst 74:711–720

Hurlburt HE, Thompson JD (1980) Numerical study of loop current intrusions and eddy shedding. J Phys Oceanogr 10:1611–1651

Lin II, Liu WT, Wu CC, Chiang JCH, Sui CH (2003) Satellite observations of modulation of surface winds by typhoon-induced upper ocean cooling. Geophys Res Lett 30(3):1131. doi:10.1029/2002GL015674

Liu CX, He XC (2003) The Analysis on the statistical character of QuikSCAT scatterometer winds and strong wind frequency using remote sensor data from QuikSCAT. J Trop Meteor 19:107–117 (in Chinese)

Liu ZY, Yang HJ, Liu QY (2001) Regional dynamics of seasonal variability in the South China Sea. J Phys Oceanogr 31:272–284

Metzger EJ, Hurlburt H (1996) Coupled dynamics of the South China Sea, Sulu Sea, and the Pacific Ocean. J Geophys Res 101:12331–12352

Metzger EJ, Hurlburt H (2001) The nondeterministic nature of Kuroshio penetration and eddy shedding in the South China Sea. J Phys Oceanogr 31:1712–1732

Qu TD (2000) Upper-layer circulation in the South China Sea. J Phys Oceanogr 30:1450–1460

Shaw PT, Chao SY, Fu LL (1999) Sea surface height variation in the South China Sea from satellite altimetry. Oceanol Acta 22(1):1–17

Su J (2004) Overview of the South China Sea circulation and its influence on the coastal physical oceanography near the Pearl River Estuary. Cont Shelf Res 24:1745–1760

Sverdrup HU (1947) Wind-driven currents in a baroclinic ocean; with application to the equatorial currents of the eastern Pacific. Proc Natl Acad Sci USA 33:318–326

Wang G, Su J, Chu PC (2003) Mesoscale eddies in the South China Sea detected from altimeter data. Geophys Res Lett 30(21). doi:10.1029/2003GL018532

Wang G, Chen D, Su J (2006) Generation and life cycle of the dipole in South China Sea summer circulation. J Geophys Res 111:C06002. doi:10.1029/2005JC003314

Wang G, Su J, Ding Y, Chen D (2007) Tropical cyclones genesis over the South China Sea. J Mar Syst 68:318–326

Wang G, Chen D, Su J (2008) Winter eddy genesis in the Eastern South China Sea due to orographic wind-jets. J Phys Oceanogr 38:726–732

Wang G, Ling Z, Wang C (2009) Influence of tropical cyclones on seasonal ocean circulation in the South China Sea. J Geophys Res 114:C10022. doi:10.1029/2009JC005302

Wang G, Wang C, Huang RX (2010) Interdecadal variability of the eastward current in the South China Sea associated with the summer Asian monsoon. J Clim 23:6115–6123

Wrytki K (1961) Scientifc results of marine investigation of the South China Sea and Gulf of Thailand. NAGA report 2

Xie SP, Xie Q, Wang DX, Liu WT (2003) Summer upwelling in the South China Sea and its role in regional climate variations. J Geophys Res 108(c8):3261. doi:10.1029/2003JC001876

Xu XZ, Qiu Z, Chen HC (1982) The general descriptions of the horizontal circulation in the South China Sea. In: Proceedings of the 1980 symposium on hydrometeorology. Chinese Society of Oceanology and Limnology, Science Press, Beijing, pp 137–145 (in Chinese)

Yin X, Wang Z, Liu Y, Xu Y (2007) Ocean response to Typhoon Ketsana traveling over the northwest Pacific and a numerical model approach. Geophys Res Lett 34:L21606. doi:10.1029/2007GL031477

Zhang QH, Fan HM, Qu YY (2006) Kuroshio intrusion into the South China Sea. J Hydro 18:702–713

Zhu DY, Li L (2007) Near inertial oscillations in shelf-break of northern South China Sea after passage of typhoon Wayne. J Trop Oceanogr 26(4):1–7